Research Square

Preprints are preliminary reports that have not undergone peer review.
They should not be considered conclusive, used to inform clinical practice,
or referenced by the media as validated information.

Early-life Staphylococcus epidermidis infection disrupts neuronal primary cilia number and signaling networks in the developing hippocampus

Maryam Ardalan

maryam.ardalan@gu.se

university of gothenburg https://orcid.org/0000-0003-3414-1584

Sofia Rasmusson
Marida Canonero
Sahar Soleimani Sani
Pernilla Svedin
Seyedeh Marziyeh Jabbari Shiadeh
Carina Mallard

Article

Keywords: Primary cilia, Neuron, Hippocampus, inflammation, Development

Posted Date: August 6th, 2026

DOI: https://doi.org/10.21203/rs.3.rs-10244030/v1

License: This work is licensed under a Creative Commons Attribution 4.0 International License.
Read Full License

Additional Declarations: There is **NO** Competing Interest.

Abstract

Background

Early-life infection is a major environmental risk factor for impaired brain development, yet the mechanisms linking neonatal infection to disrupted neurodevelopment remain poorly understood. *Staphylococcus epidermidis (SE)*, a leading cause of neonatal sepsis, may influence developmental signaling through neuronal primary cilia, sensory organelles that regulate multiple pathways essential for brain maturation. We investigated whether neonatal *SE* infection alters neuronal primary cilia and cilia-associated signaling networks in the developing hippocampus.

Methods

Hippocampal proteomic data from male mice 24 h after neonatal *SE* infection (PND5) were re-analyzed to identify cilia-associated proteins and pathways. Moreover, stereological quantification of neuronal primary cilia in hippocampal subregions was performed.

Results

SE infection induced coordinated remodeling of cilia-associated protein networks, characterized by altered expression of proteins involved in ciliary structure, cytoskeletal organization, and developmental signaling. Pathway analyses identified dysregulation of Hedgehog, Wnt, BMP/TGF-β, PKA/CREB, PDGF, and mTOR signaling. Structurally, *SE* infection increased neuronal primary cilia density in the CA1 and CA3 pyramidal layers without affecting cilia length, although region-specific alterations in the upper distribution of cilia lengths were detected.

Conclusions

These findings identify primary cilia as a sensitive target of early-life inflammation and provide a potential mechanistic link between neonatal infection and altered hippocampal development.

Introduction

The early postnatal period represents a critical window of brain development during which neural circuits are highly sensitive to environmental influences. Neonatal infection and inflammation have emerged as important risk factors for abnormal brain development and cognitive disabilities due to altered key neurodevelopmental processes, including synaptogenesis, neurogenesis and circuit formation. Sensitive brain regions, such as the hippocampus, have shown to be particularly vulnerable to postnatal immune activation, leading to disrupted synaptic plasticity ultimately affecting long-term spatial memory (1–3). In particular, infections caused by opportunistic pathogens such as *Staphylococcus epidermidis*, the

leading cause of iatrogenic late-onset neonatal sepsis, is associated brain injury following systemic inflammation (4, 5). Our previous work demonstrated that systemic neonatal *Staphylococcus epidermidis* (*SE*) infection can induce altered brain development even when direct bacterial invasion is undetectable. (4). However, despite increasing recognition of these effects, the underlying mechanisms contributing to adverse brain development associated with systemic neonatal inflammation are largely unknown.

In recent years, the primary cilium has received increasing attention due to its role as a 'cellular antenna', sensing extracellular signals and coordinating intracellular responses (6, 7). Primary cilia are solitary, sensory organelles that protrude from the cell surface of cells in the CNS. In addition to maintaining cellular homeostasis via extracellular sensing, primary cilia have proved to have a crucial regulatory role in key developmental signaling pathways, such as Hedgehog, Wnt, BMP/TGF-β, platelet-derived growth factor (PDGF), and cAMP/PKA signaling. Studies show that abnormal primary cilia function alters fundamental processes during brain development, including neuronal differentiation, migration, polarity, and circuit assembly (8, 9), suggesting that primary cilia are essential for proper brain development.

Ciliary function is heavily dependent on its unique microtuble-based structure and cytoskeletal organization – a prerequisite for intracellular transportation, which enables communication between the external environment and the cell. The assembly and maintenance of the ciliary structure depend on coordinated microtubule dynamics, intraflagellar transport (IFT), and motor protein activity, while their signaling capacity relies on the precise localization of receptors and downstream effectors (10, 11). Disruption of these processes can impair both structural stability and signal transduction, leading to widespread alterations in cellular function. Therefore, it is not surprising that inherited defects in genes encoding for ciliary proteins have proven to underlie a wide range of disorders, called "ciliopathies". Since primary cilia are located on nearly all human cells, patients with ciliopathies usually display multiorgan abnormalities, including neurological manifestations. Interestingly, more subtle irregularities in cilia-related pathways may also be linked to common neurological, neurodevelopmental and psychiatric pathologies, ranching from autism spectrum disorder (ASD) and schizophrenia to Alzheimer's and Parkinson's disease (12, 13).

Emerging evidence suggest that inflammatory signals can directly influence ciliary biology. Pro-inflammatory mediators have been shown to affect cilia length, assembly, and signaling capacity, potentially altering the ability of cells to respond to developmental cues (14, 15). In parallel, pathways known to be modulated by inflammation including cAMP/PKA, mTOR, and growth factor signaling are closely linked to ciliary function (16, 17). These observations suggest that early-life infection and the associated inflammatory response may partly disrupt cilia structure and associated signaling networks (15, 18). Simultaneously, during early postnatal development, hippocampal neurons undergo extensive structural and functional refinement, processes that are tightly regulated by intracellular signaling pathways and cytoskeletal dynamics (19). Primary cilia are well positioned to influence these processes (20), yet region-specific alterations in neuronal cilia following neonatal infection have not been investigated. In the present study, we investigated the effects of neonatal *Staphylococcus epidermidis* infection on primary cilia in the developing hippocampus by combining proteomic re-analysis with direct

structural assessment of neuronal primary cilia. Using a hypothesis-driven approach, we identified differentially expressed proteins associated with primary cilia and mapped these changes onto functional pathways and interaction networks. In parallel, we quantified neuronal cilia number and length across hippocampal subregions to determine whether structural alterations accompany the observed molecular changes. By integrating proteomic, functional, and structural analyses, this study provides a comprehensive characterization of how neonatal infection influences primary cilia in the developing brain.

Method and material

Data source and study design

Proteomic data analyzed in this study were obtained from a previously published dataset examining hippocampal protein expression 24 h after *Staphylococcus epidermidis* infection in neonatal mice. In the original study, whole hippocampi from postnatal day (PND) 5 C57Bl/6J wild-type (WT) male mice were collected following infection or saline injection and analyzed using tandem mass tag (TMT)-based quantitative proteomics (5). All animal experiments were conducted in accordance with relevant regulatory standards and approved by the Gothenburg Animal Ethical Committee (No. 663/2017).

Staphylococcus epidermidis growth

To prepare the bacteria for injection, an overnight culture was subcultured into tryptic soy broth in a vented Erlenmeyer flask on the day of infection and incubated with shaking at 37°C (240 rpm) for approximately 4 hours. The culture was then centrifuged, and the resulting pellet was resuspended in endotoxin-free saline to obtain a final concentration of 3.5×10^7 CFU of S. *epidermidis* at the desired CFU/ml.

Brain sample collection for neuronal primary cilia analysis

At PND5, male pups were deeply anesthetized by intraperitoneal injection of pentobarbital (Pentothal® Sodium) and subsequently perfused transcardially with saline. Brains were carefully removed and one hemisphere fixed by immersion in 6% buffered formaldehyde solution (Histofix, Histolab, Göteborg, Sweden) for one week, followed by cryoprotection in 30% sucrose for 48 hours. The tissue was then frozen in cold isopentane (Sigma-Aldrich, Darmstadt, Germany). Coronal brain sections (40 µm thick) with a section sampling fraction (SSF) of 1/4 were cut using a cryostat (Leica CM3050 S, Germany).

Immunohistochemistry

Free-floating 40 µm sections were processed for immunohistochemistry as previously described (21). Briefly, sections were washed in PBS, subjected to heat-induced antigen retrieval, and treated to block endogenous peroxidase activity. Tissue was then incubated overnight at 4°C with a rabbit anti-ACIII

primary antibody (EnCor Biotechnology Inc, Cat# RPCA-ACIII, 1:10.000), followed by incubation with a biotinylated secondary antibody (1:250, Vector Laboratories, Olean, NY, USA) and ABC Elite detection reagents. Immunoreactivity was visualized using DAB. Finally, sections were counterstained with thionin, dehydrated through graded ethanol, cleared in xylene, and coverslipped.

Identification of cilia-related proteins

Cilia-associated proteins were identified by cross-referencing gene symbols with five curated databases (IMCD3 proteome, CiliaCarta, SCGSv2, CilioGenics, and CiliaMiner). Proteins matching at least one resource were classified as cilia-related. Significant hits were manually curated for relevance to primary cilia, yielding a final set of 13 proteins.

Visualization and statistical analysis

Volcano plots were generated using log2FC and −log10 (P) values. Gene-level abundances were visualized using violin plots and compared between groups using the Wilcoxon rank-sum test with Cliff's delta as effect size. Heatmaps were generated using Complex Heatmap with row-scaled (z-score) data and hierarchical clustering.

Functional enrichment analysis

Gene Ontology (GO: BP, GO: CC) and Reactome pathway enrichment analyses were performed using clusterProfiler and ReactomePA, using all detected proteins with mappable gene symbols/Entrez IDs as background. Enrichment results were filtered at nominal $p < 0.05$, and terms relevant to primary cilia biology were manually selected.

Network visualization

Term–gene relationships were visualized using treeplots, category–gene networks, and chord diagrams, with gene nodes colored by log2 fold change.

Protein–protein interaction (PPI) network expansion

We performed a PPI network expansion starting from 13 primary cilia–related proteins. Differential expression data were processed at the gene level, retaining one representative entry per gene based on the largest absolute log fold change (logFC). Differential expression was defined as $p < 0.05$ and $|\text{logFC}| \geq \log_2(1.1)$. The 13 proteins were used as seed genes for STRING analysis (Mus musculus, species ID 10090). Seed proteins were mapped to STRING identifiers, and interaction partners were retrieved using a minimum confidence score of 700 (functional network), with up to 25 partners per seed. Candidate

partners were ranked based on connectivity and interaction scores, and the top 40 proteins were selected for network expansion.

The final network consisted of the 13 seed proteins and 40 selected partners. Interactions among all nodes were retrieved from STRING using the same confidence threshold. The network was integrated with differential expression data, classifying proteins as seed, differentially expressed, detected only, or PPI-expanded.

Network topology was analyzed by calculating degree, strength, betweenness, and closeness centrality (using inverse edge weights). Community structure was identified using Louvain clustering, and hub proteins were ranked based on combined centrality measures.

Pathway completion and mechanistic analysis

To contextualize the expanded network, we performed pathway completion analysis using canonical mouse gene sets from MSigDB (Reactome, KEGG Medicus, and WikiPathways). Pathways relevant to cilia biology were identified through keyword-based screening of pathway names, targeting signaling, transport, and cytoskeletal processes.

For each pathway, gene-level support was assessed by integrating seed proteins, differential expression data, and PPI-expanded partners. Pathways were scored based on the presence of seed genes, significantly altered genes, and overall dataset coverage.

Candidate pathways were grouped into major biological themes, including Hedgehog, BMP/TGF-β, Wnt, PKA/cAMP, PDGF/RTK, mTOR, ciliary trafficking, and cytoskeleton/adhesion. A representative high-support pathway was selected for each theme.

A final curated pathway panel was constructed, and genes were organized into functional modules (e.g., ligands, receptors, signaling components, trafficking machinery, cytoskeletal elements). Integration with expression and PPI data enabled classification of each gene and identification of supported and missing pathway components.

Neuronal primary cilia analysis

Quantification of primary cilia length was performed using stereological methods as previously described (21). Briefly, ACIII–thionin–stained sections were analyzed in the CA1 and CA3 pyramidal layers (CA1.P, CA3.P) and the granule cell layer (GCL) of hippocampus. Measurements were obtained using a 100× oil-immersion objective on a stereology-equipped light microscope with digital imaging and newCAST software (Visopharm).

Section thickness was determined after processing, and an optical disector height of 12 μm was applied within this thickness to correct for z-axis shrinkage, ensuring unbiased length and number estimates. Regions of interest were sampled using an area sampling fraction (ASF) of 7% for primary cilia length

measurement and 4% for counting the number of primary cilia. This 3D approach accounts for differences in cilia orientation and provides accurate structural assessment.

The density of primary cilia was calculated according to the following formula:

$$N = \Sigma Q^{-} / V$$

N reflects the total number of primary cilia per unit of volume of each brain region, ΣQ^{-} is the sum of all counted primary cilia, and V reflects the volume of each region of interest per sampling area.

Statistics

Statistical analyses of neuronal primary cilia length and number density were performed in R (v4.5.2). Between-group differences (Saline vs *SE)* were assessed for each CA1.P and GCL using independent two-sample t-tests, whereas Welch's t-test was used for CA3.P primary cilia density. Effect sizes were summarized using Cohen's d. Region-specific differences within each experimental group were evaluated using repeated-measures ANOVA with animal ID as the repeated factor, followed by paired regional comparisons without multiplicity adjustment. Associations between primary cilia length and number density were assessed using Pearson correlation analysis within each region and experimental group. Two-sided *p*-values are reported. The data are presented as mean ± SD. Violin plots show group distributions; boxes show median and IQR; white diamonds show means. A significance level of $p \leq 0.05$ was applied in all analyses.

Proteomics data processing and differential analysis

The present work represents a secondary, hypothesis-driven re-analysis of published proteomic data (5), focusing specifically on primary cilia-associated proteins and pathways. Normalized protein abundance data were imported into R (v4.5.2) and processed as described above. Analyses included 5 control and 5 *SE*-infected hippocampal samples. Values ≤ 0 were treated as missing and data were log2-transformed. Missing values were imputed using a Perseus-like left-shifted Gaussian distribution applied per sample. Differential abundance was assessed using limma with empirical Bayes moderation. Analytical thresholds differed from the original study to support targeted biological interrogation in this hypothesis-driven re analysis, with significance defined as nominal $p < 0.05$ and $|\log_2 FC| \geq \log_2(1.1)$.

Quantile analysis

Quantile analysis was performed in MATLAB R2024b (MathWorks, USA). Cilia length measurements were first stratified by experimental group (*SE* vs. saline). For each hippocampal region (CA1.P, CA3.P, and GCL), the 25th, 50th (median), and 75th percentiles were computed using MATLAB's built-in quantile function, which applies a linear interpolation method (Type 7). Quantile values were subsequently visualized to compare distributional differences between groups.

Results

Neonatal infection with Staphylococcus epidermidis induces coordinated remodeling of primary cilia–associated protein networks in the hippocampus

To characterize early changes in primary cilia–associated proteins following neonatal *Staphylococcus epidermidis* infection, we examined the magnitude and direction of protein expression differences between control and inflamed conditions (Fig. 1). Analysis of effect size distributions revealed consistent directional shifts in key cilia-associated proteins. Proteins including SLC2A1, SMAD1, SOD1, and IGF1R exhibited increased abundance in inflamed samples, with large effect sizes. In contrast, proteins including PRKAR1A, ANXA3, NME7, ANXA6, TPPP, and VCL showed consistent decreases in expression. Notably, proteins involved in microtubule dynamics displayed divergent regulation, with TUBB6 increased, while TPPP and NME7 were decreased, suggesting a shift in the balance between microtubule assembly and stabilization processes. These findings indicate an asymmetric pattern of regulation within primary cilia–associated protein networks.

To further assess the global proteomic response and statistical significance of these changes, volcano plot analysis was performed (Fig. 2A). Differential expression analysis demonstrated a clear separation between upregulated and downregulated proteins based on fold change ($\log_2$FC) and statistical significance ($-\log_{10}$ p-value). The proteins identified in the effect size analysis were also significantly altered, confirming the robustness of the observed directional changes. Among the differentially expressed proteins, a subset of primary cilia–associated proteins exhibited pronounced and directionally consistent changes. Proteins including SLC2A1, SMAD1, SOD1, IGF1R, and TUBB6 were upregulated, whereas CERS1, NME7, PRKAR1A, ANXA3, TPPP, and VCL were downregulated, indicating an asymmetric response within cilia-associated networks. Notably, SLC2A1 exhibited one of the strongest combined effects in terms of fold change and statistical significance among the labeled proteins.

To assess the consistency of these changes across samples, hierarchical clustering was performed on differentially expressed cilia-associated proteins (Fig. 2B). Samples segregated according to experimental condition, demonstrating a robust and reproducible proteomic response to neonatal inflammatory exposure. At the protein level, two distinct clusters emerged corresponding to direction of regulation. Upregulated proteins were associated with pathways linked to metabolic activity, oxidative stress, and growth factor signaling, whereas downregulated proteins were enriched for components involved in cytoskeletal organization, microtubule stability, and ciliary structure. Together, these findings establish a coordinated shift in primary cilia–associated protein expression following neonatal infection.

Functional enrichment analysis links structural remodeling of cilia to altered signaling and vascular-associated processes

To determine the functional implications of these proteomic changes, gene ontology and pathway enrichment analyses were performed on differentially expressed cilia-associated proteins (Fig. 3; Fig. 4). Gene Ontology biological process analysis revealed significant enrichment of pathways related to

microtubule cytoskeleton organization, including microtubule polymerization, intracellular transport, and microtubule-based transport. In addition, processes related to tubulin post-translational modification and cAMP/PKA signaling were enriched, indicating a link between cytoskeletal dynamics and intracellular signaling regulation. Notably, pathways associated with angiogenesis and endothelial development, including regulation of sprouting angiogenesis and endothelial cell differentiation were enriched following neonatal inflammatory exposure. These findings suggest that early-life inflammation also affects vascular and barrier-associated processes, potentially contributing to alterations in blood–brain barrier function.

Cellular component analysis further demonstrated enrichment of proteins localized to key ciliary and cytoskeletal structures, including the axoneme, ciliary plasma, centrosome, and microtubule organizing center, as well as axonemal microtubule substructures and the gamma-tubulin ring complex. These findings indicate that the observed proteomic changes involve core structural elements required for ciliogenesis and microtubule organization.

Reactome pathway analysis revealed enrichment of signaling pathways closely associated with primary cilia function, including PKA/CREB signaling, Hedgehog signaling, BMP signaling, and IGF1R-mediated pathways. These pathways represent key regulators of cilia-dependent signal transduction and neurodevelopment.

Together, these analyses demonstrate that neonatal infection is associated with coordinated alterations in both the structural framework and signaling functions of primary cilia, as well as processes linked to vascular regulation in the hippocampus.

Network analysis identifies key hub proteins linking structural and signaling alterations after postnatal SE infection

To define how individual proteins, contribute to these functional changes, gene–concept network (Cnet) analysis was performed across GO-BP, GO-CC, and Reactome datasets **(**Fig. 5**)**. Within biological processes, proteins such as NME7 and TPPP emerged as central nodes connecting multiple terms related to microtubule organization and intracellular transport, indicating their role as key structural regulators. In contrast, proteins including SMAD1 and PRKAR1A showed more selective associations with signaling and developmental pathways, including angiogenesis and cAMP/PKA signaling. SLC2A1 and IGF1R were primarily linked to brain development and growth factor–related responses, suggesting more specialized functional roles.

At the level of cellular components, NME7 functioned as a highly connected structural hub linking multiple ciliary compartments, including the axoneme, centrosome, and microtubule-organizing centers, whereas other proteins displayed more restricted localization patterns.

Reactome network analysis further demonstrated that pathway enrichment was driven by a limited number of key proteins. PRKAR1A acted as a central node linking cAMP/PKA and CREB signaling

pathways, IGF1R was associated with growth factor signaling cascades, and SMAD1 was selectively connected to BMP-related developmental pathways.

These findings indicate that a small number of hub proteins coordinate the integration of structural and signaling pathways within primary cilia–associated networks, linking cytoskeletal remodeling to altered intracellular signaling following neonatal infection.

PPI network expansion reveals a central hub-dominated module and distinct peripheral clusters

To extend the 13 primary cilia–associated proteins into a broader interaction context, we constructed a high-confidence STRING-based PPI network (score ≥ 0.7), resulting in an expanded network comprising seed proteins and top-ranked interaction partners. The resulting network exhibited a clear modular structure, with a large, densely connected central component and several smaller peripheral clusters (**Figure. 6A**). The network reveals a densely connected central module in which IGF1R occupies a prominent, highly connected position, linking multiple interaction partners, while proteins such as PRKAR1A and CTNNB1 also display relatively high connectivity within the core network. In contrast, several smaller peripheral clusters are observed. These hubs bridged signaling and structural components, suggesting integration of growth factor signaling, cAMP/PKA pathways, and cytoskeletal organization within the cilia-associated network. In contrast, several proteins displayed more restricted connectivity, forming smaller clusters that likely represent functionally specialized modules. For example, a distinct cluster centered on PCNA indicates potential links to cell cycle–related processes, while smaller modules containing proteins such as NME7 and TPPP were associated with microtubule-related functions.

Louvain clustering further highlighted the modular organization of the network, identifying multiple clusters with varying sizes and compositions. The largest clusters were enriched for both seed proteins and detected proteins, whereas smaller clusters were primarily composed of PPI-expanded nodes (Fig. 6.**B**). Notably, the majority of differentially expressed proteins were concentrated within the main connected component, indicating that the most transcriptionally responsive elements are embedded within the core interaction network.

Pathway-level alterations in cilia-associated signaling following postnatal SE infection

Proteomic analysis of hippocampal tissue collected 24 hours after postnatal infection revealed differential abundance of proteins across multiple pathways associated with primary cilia structure and signaling (Fig. 7).

Within the BMP/TGF-β pathway (Fig. 7.**A**), several downstream components, including SMAD-related proteins, exhibited measurable changes, suggesting disruption of canonical developmental signaling linked to ciliary function. While many upstream ligands and regulators were not detected in the dataset.

In the ciliary trafficking pathway (Fig. 7.**B**), alterations were observed in proteins involved in IFT and motor-associated components, suggesting potential modulation of cilia-related transport processes. Key IFT components showed predominantly reduced abundance, supporting a disruption in cilia maintenance mechanisms.

The cytoskeleton and adhesion pathway (Fig. 7.**C**) showed differential abundance of proteins related to adhesion complexes and microtubule organization, indicating changes in structural components that may influence ciliary architecture.

In the Hedgehog signaling pathway (Fig. 7.**D**), selected core and downstream proteins displayed changes in abundance, while several upstream elements were not detected, suggesting impaired pathway activation. Similarly, proteins associated with the mTOR pathway (Fig. 7.**E**) showed modulation of both upstream regulators and downstream effectors, indicating altered cellular growth and metabolic signaling, which are known to influence ciliogenesis and ciliary function.

In the PDGF receptor tyrosine kinase (PDGF-RTK) pathway (Fig. 7.**F**) multiple adaptor proteins and downstream signaling components were differentially expressed, suggesting disrupted growth factor signaling at the level of primary cilia.

The PKA/cAMP pathway (Fig. 7.**G**) demonstrated changes in multiple signaling proteins, including core kinase components and downstream effectors, indicating altered cAMP-mediated signaling, a key regulator of ciliary signaling dynamics.

In the Wnt signaling pathway (Fig. 7.**H**), differential abundance was observed among core signaling proteins and planar cell polarity related proteins, further supporting widespread disruption of cilia-dependent developmental pathways.

Overall, these findings indicate that postnatal infection with *SE* is associated with changes in the abundance of multiple proteins linked to cilia-associated signaling pathways, including trafficking, cytoskeletal organization, and key developmental signaling cascades. These pathway-level alterations suggest that early-life inflammatory exposure may impair primary cilia structure and function through combined effects on trafficking, cytoskeletal organization, and signal transduction. However, the incomplete detection of pathway components suggests that these results reflect partial pathway modulation rather than comprehensive pathway activation or suppression.

Integrated gene–pathway network reveals coordinated cilia-associated signaling across multiple pathways following postnatal SE infection

To obtain a systems-level overview of cilia-associated signaling alterations following postnatal infection, differentially abundant proteins were integrated into a refined gene–pathway network encompassing key cilia-related signaling pathways (Fig. 8).

The network analysis (Fig. 8.**A**) demonstrates that several proteins were linked to more than one pathway, reflecting the interconnected nature of cilia-associated signaling networks. Notably, core signaling mediators (e.g., SMADs, kinases, and cytoskeletal regulators) were shared across pathways, highlighting convergence between developmental signaling, intracellular transport, and structural regulation. To further evaluate pathway representation within the dataset, we quantified the detection status of pathway components (Fig. 8.**B**). Across all pathways, a substantial proportion of components were not detected in the proteomic dataset, indicating incomplete pathway coverage. Among detected proteins, the majority were classified as “detected only,” with a smaller fraction identified through PPI expansion or as predefined seed components. Pathway-specific differences in coverage were observed. The ciliary trafficking and mTOR pathways showed relatively higher proportions of detected components, suggesting broader representation in the dataset. In contrast, pathways such as BMP/TGF-β and Wnt contained a larger number of missing components, reflecting more limited detection of upstream ligands and signaling elements. The cytoskeleton/adhesion and PDGF-RTK pathways exhibited a mixed profile, with contributions from both directly detected proteins and PPI-expanded components.

Overall, this integrative analysis indicates that postnatal *SE* infection–associated proteomic changes are distributed across multiple, functionally interconnected cilia-related pathways.

Changes in the hippocampal neuronal primary cilia number density and length following neonatal Staphylococcus epidermidis infection

To characterize changes in hippocampal neuronal primary cilia following neonatal *SE* infection, we examined differences in the number density and length of primary cilia between control and *SE* infected conditions. We found a significant increase in the number density of primary cilia in *SE* infected mice compared with controls in both CA1.P ($t_{(8)}$=-2.36, p = 0.045) and CA3.P ($t_{(6.07)}$=-2.69, p = 0.036) subregions of hippocampus, while no significant difference was observed in GCL ($t_{(8)}$=-0.46, p = 0.655). These findings were further supported by the analysis of the effect size distributions, which confirmed a robust effect of *SE* infection on the number density of primary cilia in CA1.P (d = 1.50) and CA3.P (d = 1.70), while just a very small effect was detected in GCL (Fig. 9.**A-C**).

In contrast, the primary cilia length was not affected by *SE* infection in any of the regions analyzed (CA1.P: $t_{(8)}$=-0.001, p = 0.999; CA3.P: $t_{(8)}$ = 0.30, p = 0.768; GCL: $t_{(8)}$ = 1.22, p = 0.255), suggesting that the inflammation primarily acts on the primary cilia number rather than length (Fig. 9.**D**).

In the next step, we assessed the correlation between cilia number and length across hippocampal regions, but we did not observe any significant correlation in either the control group (CA1.P: r=-0.340, p = 0.571; CA3.P: r=-0.021, p = 0.973; GCL: r = 0.017, p = 0.978), inflamed group (CA1.P: r = 0.410, p = 0.491; CA3.P: r=-0.740, p = 0.157; GCL: r = 0.760, p = 0.136), suggesting that these two parameters independent from each other are affected by the postnatal infection with *SE* (Fig. 9.**E**).

However, from the analysis of the effect size distributions, a moderate effect on neuronal primary cilia length in GCL was detected (d = 0.78), whereas in CA1.P and CA3.P the effects were small.

To assess the region-specific effects of *SE* infection on neuronal primary cilia, we analyzed regional differences in primary cilia length and number density in control and inflamed groups. In both conditions, CA3.P region displayed significantly longer cilia than CA1.P (Saline: $p = 0.005$; *SE*: $p = 0.019$) and GCL (Saline: $p < 0.001$; *SE*: $p < 0.001$), whereas in GCL the cilia were, on average, significantly shorter than in CA1.P in both groups (Saline: $p < 0.001$; *SE*: $p < 0.001$) (Fig. 10.**A**).

Regarding the number density of neuronal primary cilia, in the saline group, no significant differences in primary cilia density were observed between CA1.P, CA3.P, and GCL regions ($p > 0.05$). In contrast, the *SE* group demonstrated significant regional variation in primary cilia density. Primary cilia density was significantly higher in CA1.P compared with CA3.P ($p = 0.049$) and GCL ($p = 0.006$), whereas the difference between CA3.P and GCL did not reach statistical significance ($p = 0.121$). These findings indicate that neonatal *SE* exposure alters the regional distribution of primary cilia density within the hippocampus, with the highest density observed in the CA1.P (Fig. 10.**B**).

Quantile analysis revealed region-specific differences in primary cilia length between saline and *SE* groups in the hippocampus. In the CA1.P, primary cilia length in the *SE* group was higher at the 25th and 50th percentiles compared with saline, whereas the 75th percentile was lower in *SE* than in saline, indicating reduced upper-range cilia lengths following *SE* infection. In the CA3.P, the *SE* group showed consistently shorter cilia lengths across the 50th and 75th percentiles relative to saline, while the 25th percentile was slightly increased. In the GCL, differences between groups were minimal at the lower and median quantiles, but the 75th percentile was markedly reduced in the *SE* group compared with saline, suggesting attenuation of the longest cilia population after *SE*.

Overall, the quantile-based approach demonstrated that *SE*-associated alterations were not uniformly distributed across the population of primary cilia lengths, with the strongest effects observed in the upper quantiles, particularly in CA3.P and GCL (Fig. 10.**C**).

Discussion

A growing body of evidence indicates that perinatal and early postnatal infections can alter neurodevelopment through persistent effects on immune signaling, synaptic maturation, and the neuroimmune axis, with long-term consequences for brain organization and behavior (3, 22). The immature brain undergoes rapid structural changes during this period and inflammatory insults may disrupt developmental programs that normally guide differentiation, connectivity, and circuit stabilization (23, 24). However, to what extent postnatal immune activation contributes to altered neurodevelopment remains largely unknown, highlighting the need to identify vulnerable subcellular systems including primary cilia.

In the present study, we show that neonatal *SE* infection is associated with coordinated remodeling of hippocampal primary cilia–related protein networks. Importantly, our results show a selective increase in primary cilia number density in CA1 and CA3 pyramidal layers. Unexpectedly, however, cilia length remained unchanged in all regions, suggesting that infection influences cilia abundance or maintenance

rather than morphology. Together, these findings support the concept that primary cilia function as a sensitive developmental interface through which inflammatory signals can influence hippocampal maturation during a critical postnatal window.

Coordinated cilia-network remodeling

The proteomic data revealed an asymmetric response within the cilia-associated protein landscape after neonatal *SE* infection. While our results showed an increase of proteins involved in developmental signaling and growth (e.g., IGF1R, SMAD1, SLC2A1, and SOD1), there was a reduction in proteins supporting cilia structures, such as microtubule stability, intracellular organization, and ciliary architecture, (e.g. PRKAR1A, NME7, TPPP, ANXA3, ANXA6, and VCL).

The biological significance of this pattern may lie in the structural and signaling hubs. For instance, reduction of centrosomal and microtuble associated proteins such as NME7 and TPPP (25) (26) may represent a disruption of ciliary scaffold and impaired downstream receptor trafficking under conditions of inflammation. Similarly, the observed increase in cilia-dependent growth factor proteins, e.g., IGF1 and SMAD1, which regulate differentiation and survival, reflects the upregulation of developmental signals typically triggered by inflammation (27–31). Likewise, the detected increase in SLC2A1 and SOD1 may indicate metabolic and oxidative stress adaptations, solidifying the crucial role of primary cilia in a broader context of cellular remodeling during inflammation (32–36). Together, these findings support a model in which neonatal inflammation shifts the balance from structural maintenance of primary cilia toward adaptive signaling responses, potentially altering how developing neurons perceive and integrate extracellular developmental cues. Such alterations may have important consequences for neuronal maturation, circuit formation, and long-term hippocampal function, potentially contributing neurodevelopmental disorders associated with neonatal inflammation (3).

The network-based analyses further supported this interpretation. Central hub proteins such as NME7, TPPP, PRKAR1A, SMAD1, and IGF1R connected multiple functional categories, indicating that a relatively limited number of proteins may coordinate broader cilia-associated responses to inflammatory exposure. The enrichment of these hubs within structural and signaling terms suggests that the ciliary response is integrated across cytoskeletal organization, receptor-mediated signaling, and developmental pathway regulation rather than occurring as isolated molecular changes. This is consistent with the established role of primary cilia as signaling hubs that organize pathway specificity through precise trafficking and compartmentalization of receptors and downstream effectors (6).

Signaling and structural implications

Functional enrichment analyses showed that proteins altered by neonatal *SE* infection were upregulated in pathways related to microtubule organization, intracellular transport, tubulin post-translational modification, and cAMP/PKA signaling. Interestingly, primary cilia depend on microtubule scaffold and IFT to maintain structural integrity and signal transduction capacity (8, 37). The observed

downregulation of ciliary proteins, together with upregulation of growth factor and signaling proteins, may reflect a shift from structural maintenance to inflammatory or compensatory signaling.

The Hedgehog, BMP/TGF-β, Wnt, PDGF-RTK, and mTOR-related pathways are central regulators of neurodevelopment and are known to interact with ciliary receptors, particularly during neuronal differentiation, polarity establishment, and circuit formation (8, 38, 39). In the developing hippocampus, where postnatal maturation depends on tightly regulated signaling and cytoskeletal remodeling, disruption of these pathways could plausibly have lasting consequences for neuronal organization and function (19, 40).

An additional notable finding is the enrichment of vascular- and endothelial-related cilia-associated proteins. These findings suggest that primary cilia may also be involved in regulation of neurovascular development. Therefore, disruption of cilia-related signaling may not only contribute to neuronal structural changes but also to altered blood-brain barrier maturation(41–43).This interpretation is consistent with the notion that early inflammation can produce multi-compartmental effects rather than isolated neuronal changes (44). Moreover, cilia are also expressed on non-neuronal brain cells, including astrocytes and microglia, it is possible that the proteomic changes observed in this study reflect contributions from multiple cell types in the hippocampal tissue (45–47). This possibility broadens the biological significance of the findings and suggests that cilia-centered responses to infection may operate across cellular compartments.

Region-specific hippocampal effects

A major structural finding of this study was the selective increase in neuronal primary cilia density in the CA1.P and CA3.P following neonatal *SE* infection, with no detectable change in cilia length. The results suggest that neonatal *SE* infection in an acute phase influences ciliogenesis, cilia maintenance, and the proportion of ciliated neurons, but does not affect ciliary length. In fact, our results indicate that these two parameters – cilia number and cilia length – are independently regulated and react differently to inflammatory stress.

The dynamic nature of primary cilia prerequisites a fast-adaptive response (21, 48). The observed increased cilia density in response to inflammatory stress may therefore represent an adaptive response to inflammatory stress, potentially enhancing the ability of developing neurons to detect and integrate extracellular signals during a period of environmental challenge. Alternatively, inflammatory signaling may alter the balance between cilia assembly and resorption, resulting in a greater proportion of neurons retaining primary cilia.

Region-specific differences in primary cilia density, with the highest primary cilia density was observed in CA1.P after *SE* infection. During early postnatal periods, CA1 and CA3 pyramidal neurons undergo extensive structural maturation and synaptic refinement. and may therefore be particularly sensitive to inflammatory perturbations (49), which may reflect the intrinsic differences across hippocampal

subfields associated with developmental timing, neuronal composition, and signaling requirements. Such regional selectivity may also have implications for circuit refinement and later cognitive function.

Interestingly, the data also pointed towards regional variation in neuronal primary cilia length across hippocampal subregions. In both experimental groups, CA3 pyramidal neurons exhibited longer primary cilia than CA1 pyramidal neurons, whereas neurons within the GCL displayed the shortest cilia. These findings suggest that primary cilia length is tightly linked to regional neuronal identity and is regulated according to the specific functional and developmental requirements of each hippocampal subfield. Since primary cilia serve as specialized signaling compartments, differences in cilia length may be associated with variations in receptor composition, signaling capacity, and responsiveness to extracellular cues (50, 51). In this case, longer cilia were observed in CA3 pyramidal neurons, which may reflect greater signaling demands in the region, which is characterized by extensive recurrent connectivity and plays a central role in hippocampal information processing. In contrast, the GCL displayed shorter cilia, which may be related to the distinct cellular composition and signaling requirements of dentate granule neurons. Importantly, these regional differences were preserved following neonatal *SE* infection, suggesting that the intrinsic patterning of cilia morphology across hippocampal subregions is most likely established early and remains relatively stable despite inflammatory exposure. Therefore, our data establish that primary cilia are regionally specific. However, whether there are functional differences between cilia in the observed hippocampal subregions needs further investigations.

The quantile-based analysis provided additional insight by showing that infection did not shift the entire cilia-length distribution uniformly, but instead affected the upper range of lengths particularly in CA3.P and the GCL, where reductions were most evident at the 75th percentile. This pattern suggests that longer cilia may be more vulnerable to inflammatory perturbation during early brain development than shorter cilia. In contrast, CA1.P displayed a more complex response, with modest increases in cilia length at lower and intermediate quantiles but shorter cilia at the upper quantile. This suggests that inflammatory exposure may selectively influence a subset of cilia populations rather than producing a global uniform effect. Such non-uniform changes could reflect differences in neuronal subtype, developmental stage, or local microenvironmental sensitivity within the hippocampus.

Limitations and perspective

Some limitations should be considered in this study. First, the proteomic analysis was performed on whole hippocampal tissue, which limits cell type-specific resolution and may obscure localized responses within distinct neuronal or glial populations. Second, the pathway analyses reflect partial coverage of the proteome, and many upstream components were not detected, so pathway reconstruction should be interpreted as supportive rather than exhaustive. Third, the structural analysis was restricted to a single early time point, preventing conclusions about the persistence, progression, or reversibility of the cilia changes.

Conclusion

In summary, neonatal *Staphylococcus epidermidis* infection is associated with coordinated remodeling of hippocampal cilia-related protein networks. Additionally, a selective increase in neuronal primary cilia density in specific hippocampal subregions were observed. The combined proteomic and structural data suggest that primary cilia are a vulnerable developmental target of early-life inflammation and may represent an important mechanistic bridge between neonatal infection, signaling disruption, and altered hippocampal maturation. These findings provide a foundation for future studies aimed at defining the causal role of ciliary dysfunction in inflammation-associated neurodevelopmental vulnerability.

Declarations

Conflict of Interest Statement

The authors declare that they have no competing interests.

Funding Sources

This study was supported by the Swedish Research Council (2023–02602, MA), Styrelsen för Wilhelm och Martina Lundgrens Vetenskapsfond (2025-SA-4895, MA), Swedish Research Council (2021 – 01872, CM), ALFGBG-1005755 (CM), Åhlen Foundation (243041, CM), Brain Foundation (FO2024-0049-TK-142, CM) and Jane and Dan Olsson (2025–081639, CM).

Author Contributions

SR, MA, MC and CM contributed to the study idea and design. SR, SMJSH, MC, PS and MA contributed to data collection and analysis. Bioinformatic analysis has been done by SSS. Interpretation of results and writing the draft of the manuscript were done by SR, MC, SSS, SMJSH, CM and MA. All authors were involved in the revision of the manuscript. All authors read and approved the final manuscript.

Acknowledgment:

We would like to thank Dr. Tetyana Chumak and Dr. Giacomo Gravina for their valuable assistance with tissue collection and sample processing.

Data Availability Statement

Derived data supporting the findings of this study are available from the corresponding author on request.

References

1. Malave, L., van Dijk, M.T., Anacker, C.: Early life adversity shapes neural circuit function during sensitive postnatal developmental periods. Transl Psychiatry. **12**(1), 306 (2022)
2. Chau, V., Brant, R., Poskitt, K.J., Tam, E.W.Y., Synnes, A., Miller, S.P.: Postnatal infection is associated with widespread abnormalities of brain development in premature newborns. Pediatr. Res. **71**(3), 274–279 (2012)
3. Ardalan, M., Chumak, T., Quist, A., Hermans, E., Rafati, A.H., Gravina, G., et al.: Reelin cells and sex-dependent synaptopathology in autism following postnatal immune activation. Brit J. Pharmacol. (2022)
4. Chan, W.K., Jabbari Shiadeh, S.M., Lenzig, J., Svedin, P., Rasmusson, S., Vigne, O., et al.: Immune Synaptopathy and Sex Differences in Recognition Memory from Neonatal <italic>Staphylococcus epidermidis</italic> Infection. Dev. Neurosci. :1–25. (2025)
5. Gravina, G., Ardalan, M., Chumak, T., Nilsson, A.K., Ek, J.C., Danielsson, H., et al.: Proteomics identifies lipocalin-2 in neonatal inflammation associated with cerebrovascular alteration in mice and preterm infants. iScience. **26**(7), 107217 (2023)
6. Li, B., He, Y.Y., Yang, Z.M.: Primary cilia function as hubs for signal transduction. Cell. Biosci. **15**(1), 163 (2025)
7. Lee, J.H., Gleeson, J.G.: The role of primary cilia in neuronal function. Neurobiol. Dis. **38**(2), 167–172 (2010)
8. Anvarian, Z., Mykytyn, K., Mukhopadhyay, S., Pedersen, L.B., Christensen, S.T.: Cellular signalling by primary cilia in development, organ function and disease. Nat. Rev. Nephrol. **15**(4), 199–219 (2019)
9. Stoufflet, J., Caille, I.: The Primary Cilium and Neuronal Migration. Cells ;**11**(21). (2022)
10. Christensen, S.T., Clement, C.A., Satir, P., Pedersen, L.B.: Primary cilia and coordination of receptor tyrosine kinase (RTK) signalling. J. Pathol. **226**(2), 172–184 (2012)
11. Ge, R., Cao, M., Chen, M., Liu, M., Xie, S.: Cytoskeletal networks in primary cilia: Current knowledge and perspectives. J. Cell. Physiol. **237**(11), 3975–3983 (2022)
12. Karalis, V., Donovan, K.E., Sahin, M.: Primary Cilia Dysfunction in Neurodevelopmental Disorders beyond Ciliopathies. J. Dev. Biol. ;**10**(4). (2022)
13. Valente, E.M., Rosti, R.O., Gibbs, E., Gleeson, J.G.: Primary cilia in neurodevelopmental disorders. Nat. Rev. Neurol. **10**(1), 27–36 (2014)
14. Kumari, A., Caliz, A.D., Yoo, H.J., Kant, S., Vertii, A.: TNF-alpha promotes cilia elongation via mixed lineage kinases signaling in mouse fibroblasts and human RPE-1 cells. Cytoskeleton (Hoboken). **81**(11), 639–647 (2024)
15. Mc Fie, M., Koneva, L., Collins, I., Coveney, C.R., Clube, A.M., Chanalaris, A., et al.: Ciliary proteins specify the cell inflammatory response by tuning NFkappaB signalling, independently of primary cilia. J. Cell. Sci. ;**133**(13). (2020)

16. Jiang, J.Y., Falcone, J.L., Curci, S., Hofer, A.M.: Direct visualization of cAMP signaling in primary cilia reveals up-regulation of ciliary GPCR activity following Hedgehog activation. Proc. Natl. Acad. Sci. U S A. **116**(24), 12066–12071 (2019)
17. Pedersen, L.B., Rosenbaum, J.L.: Intraflagellar transport (IFT) role in ciliary assembly, resorption and signalling. Curr. Top. Dev. Biol. **85**, 23–61 (2008)
18. Wann, A.K., Knight, M.M.: Primary cilia elongation in response to interleukin-1 mediates the inflammatory response. Cell. Mol. Life Sci. **69**(17), 2967–2977 (2012)
19. Jabes, A., Lavenex, P.B., Amaral, D.G., Lavenex, P.: Postnatal development of the hippocampal formation: a stereological study in macaque monkeys. J. Comp. Neurol. **519**(6), 1051–1070 (2011)
20. Ishii, S., Sasaki, T., Mohammad, S., Hwang, H., Tomy, E., Somaa, F., et al.: Primary cilia safeguard cortical neurons in neonatal mouse forebrain from environmental stress-induced dendritic degeneration. Proc. Natl. Acad. Sci. U S A ;**118**(1). (2021)
21. Rasmusson, S., Shiadeh, S.M.J., Dada, N., Akesson, E., Mallard, C., Ardalan, M.: Three-dimensional approaches to measuring primary cilia in hippocampal neurons: A comparative analysis. J. Neuropathol. Exp. Neurol. (2026)
22. Ardalan, M., Chumak, T., Vexler, Z., Mallard, C.: Sex-Dependent Effects of Perinatal Inflammation on the Brain: Implication for Neuro-Psychiatric Disorders. Int. J. Mol. Sci. ;**20**(9). (2019)
23. Bland, S.T., Beckley, J.T., Young, S., Tsang, V., Watkins, L.R., Maier, S.F., et al.: Enduring consequences of early-life infection on glial and neural cell genesis within cognitive regions of the brain. Brain Behav. Immun. **24**(3), 329–338 (2010)
24. Chumak, T., Jullienne, A., Ek, C.J., Ardalan, M., Svedin, P., Quan, R., et al.: Maternal n-3 enriched diet reprograms the offspring neurovascular transcriptome and blunts inflammation induced by endotoxin in the neonate. J. Neuroinflammation. **21**(1), 199 (2024)
25. Liu, P., Choi, Y.K., Qi, R.Z.: NME7 is a functional component of the gamma-tubulin ring complex. Mol. Biol. Cell. **25**(13), 2017–2025 (2014)
26. Lehotzky, A., Tirian, L., Tokesi, N., Lenart, P., Szabo, B., Kovacs, J., et al.: Dynamic targeting of microtubules by TPPP/p25 affects cell survival. J. Cell. Sci. **117**(Pt 25), 6249–6259 (2004)
27. Yeh, C., Li, A., Chuang, J.Z., Saito, M., Caceres, A., Sung, C.H.: IGF-1 activates a cilium-localized noncanonical Gbetagamma signaling pathway that regulates cell-cycle progression. Dev. Cell. **26**(4), 358–368 (2013)
28. Lindbæk, L., Warzecha, C., Koefoed, K., Mogensen, J., Schmid, F., Pedersen, L., et al.: Coordination of TGFβ/BMP signaling is associated with the primary cilium. Cilia. **4**(Suppl 1), P17 (2015)
29. Vion, A.C., Alt, S., Klaus-Bergmann, A., Szymborska, A., Zheng, T., Perovic, T., et al.: Primary cilia sensitize endothelial cells to BMP and prevent excessive vascular regression. J. Cell. Biol. **217**(5), 1651–1665 (2018)
30. Li, B., He, Y.Y., Yang, Z.M.: Primary cilia function as hubs for signal transduction. Cell. Bioscience ;**15**(1). (2025)

31. Liu, J., Leng, F.F., Gao, Y.H., He, W.F., Wang, J.F., Xian, C.J., et al.: Protection of primary cilia is an effective countermeasure against the impairment of osteoblast function induced by simulated microgravity. J. Cell. Mol. Med. **27**(1), 36–51 (2023)
32. Mahoney, D.J., Kaczor, J.J., Bourgeois, J., Yasuda, N., Tarnopolsky, M.A.: Oxidative stress and antioxidant enzyme upregulation in SOD1-G93A mouse skeletal muscle. Muscle Nerve. **33**(6), 809–816 (2006)
33. Freemerman, A.J., Zhao, L., Pingili, A.K., Teng, B., Cozzo, A.J., Fuller, A.M., et al.: Myeloid Slc2a1-Deficient Murine Model Revealed Macrophage Activation and Metabolic Phenotype Are Fueled by GLUT1. J. Immunol. **202**(4), 1265–1286 (2019)
34. Carri, M.T., Valle, C., Bozzo, F., Cozzolino, M.: Oxidative stress and mitochondrial damage: importance in non-SOD1 ALS. Front. Cell. Neurosci. **9**, 41 (2015)
35. Ma, X.X., Peterson, R., Turnbull, J.: Adenylyl Cyclase type 3, a marker of primary cilia, is reduced in primary cell culture and in lumbar spinal cord in situ in G93A SOD1 mice. BMC Neurosci. ;**12**. (2011)
36. De Decker, M., Zelina, P., Moens, T.G., Beckers, J., Contardo, M., Dittlau, K.S., et al.: C21ORF2 mutations point towards primary cilia dysfunction in amyotrophic lateral sclerosis. Brain. **148**(3), 803–816 (2024)
37. Stoufflet, J., Chaulet, M., Doulazmi, M., Fouquet, C., Dubacq, C., Metin, C., et al.: Primary cilium-dependent cAMP/PKA signaling at the centrosome regulates neuronal migration. Sci. Adv. ;**6**(36). (2020)
38. Zhang, R., Pan, S., Zhao, J., Wang, J., Yang, X., Qi, Z.: Primary cilia in neural development and disease. Neurobiol. Dis. **217**, 107184 (2025)
39. Guo, J., Otis, J.M., Higginbotham, H., Monckton, C., Cheng, J., Asokan, A., et al.: Primary Cilia Signaling Shapes the Development of Interneuronal Connectivity. Dev. Cell. **42**(3), 286–300 (2017). e4
40. Avila, J., Sousa, M.M., Sayas, C.L.: Editorial: Shaping the Brain by Neuronal Cytoskeleton: From Development to Disease and Degeneration. Front. Cell. Neurosci. **14**, 12 (2020)
41. Kugler, E.C., Greenwood, J., MacDonald, R.B.: The Neuro-Glial-Vascular Unit: The Role of Glia in Neurovascular Unit Formation and Dysfunction. Front. Cell. Dev. Biol. **9**, 732820 (2021)
42. Shiadeh, S.M.J., Goretta, F., Svedin, P., Jansson, T., Mallard, C., Ardalan, M.: Long-term impact of maternal obesity on the gliovascular unit and ephrin signaling in the hippocampus of adult offspring. J. Neuroinflammation. **21**(1), 39 (2024)
43. Ardalan, M., Chumak, T., Quist, A., Jabbari Shiadeh, S.M., Mallard, A.J., Rafati, A.H., et al.: Sex dependent glio-vascular interface abnormality in the hippocampus following postnatal immune activation in mice. Dev. Neurosci. (2022)
44. Gravina, G., Ardalan, M., Chumak, T., Rydbeck, H., Wang, X., Ek, C.J., et al.: Transcriptome network analysis links perinatal Staphylococcus epidermidis infection to microglia reprogramming in the immature hippocampus. Glia. **71**(9), 2234–2249 (2023)

45. Armato, U., Chakravarthy, B., Pacchiana, R., Whitfield, J.F.: Alzheimer's disease: an update of the roles of receptors, astrocytes and primary cilia (review). Int. J. Mol. Med. **31**(1), 3–10 (2013)
46. Tereshko, L., Turrigiano, G.G., Sengupta, P.: Primary cilia in the postnatal brain: Subcellular compartments for organizing neuromodulatory signaling. Curr. Opin. Neurobiol. **74**, 102533 (2022)
47. Ki, S.M., Jeong, H.S., Lee, J.E.: Primary Cilia in Glial Cells: An Oasis in the Journey to Overcoming Neurodegenerative Diseases. Front. Neurosci. **15**, 736888 (2021)
48. Breunig, J.J., Sarkisian, M.R., Arellano, J.I., Morozov, Y.M., Ayoub, A.E., Sojitra, S., et al.: Primary cilia regulate hippocampal neurogenesis by mediating sonic hedgehog signaling. Proc. Natl. Acad. Sci. U S A. **105**(35), 13127–13132 (2008)
49. Zhao, L., Witter, M.P., Palomero-Gallagher, N.: Cyto-, gene, and multireceptor architecture of the early postnatal mouse hippocampal complex. Prog Neurobiol. **245**, 102704 (2025)
50. Nishimura, Y., Kasahara, K., Shiromizu, T., Watanabe, M., Inagaki, M.: Primary Cilia as Signaling Hubs in Health and Disease. Adv. Sci. (Weinh). **6**(1), 1801138 (2019)
51. Macarelli, V., Leventea, E., Merkle, F.T.: Regulation of the length of neuronal primary cilia and its potential effects on signalling. Trends Cell. Biol. **33**(11), 979–990 (2023)

Figures

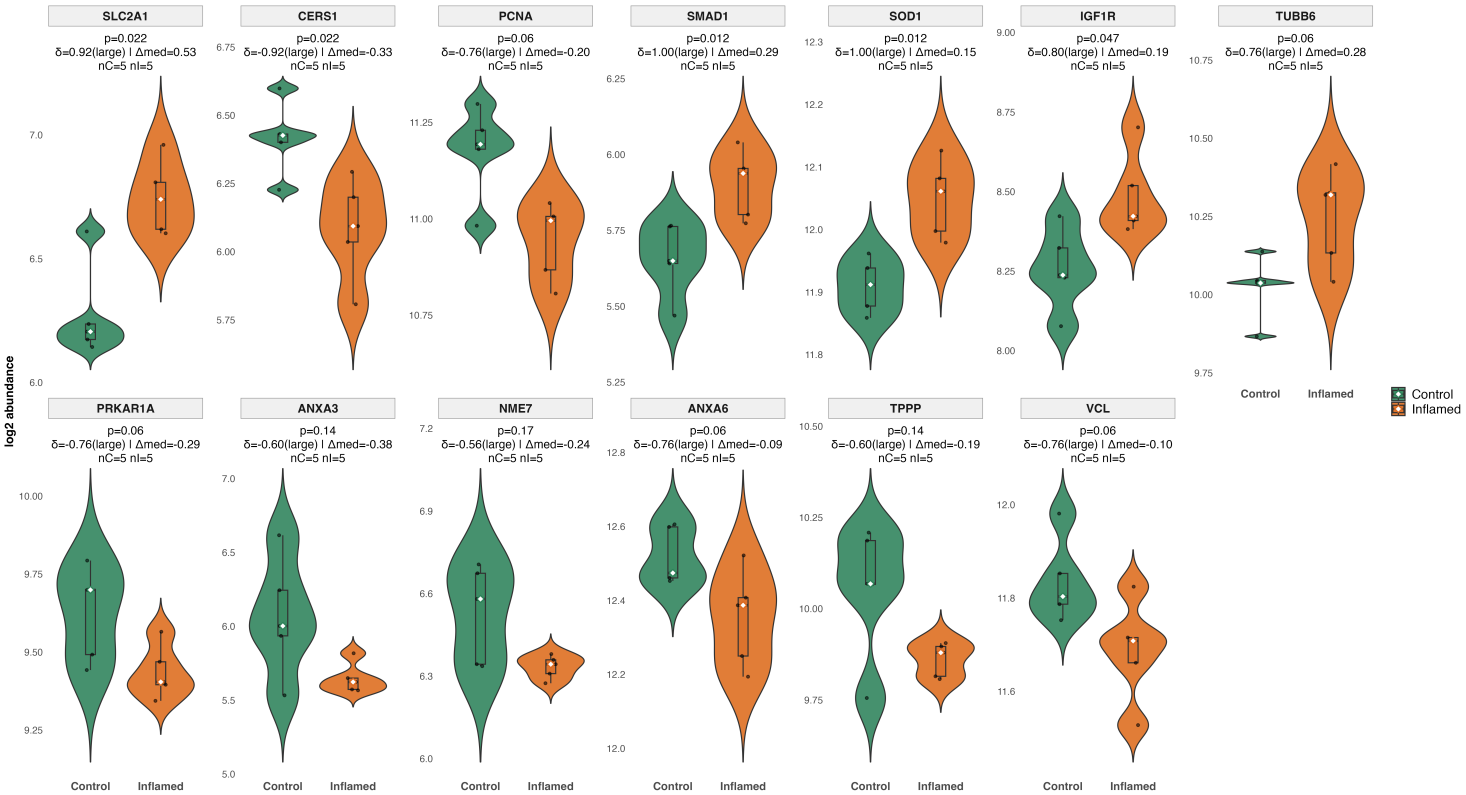


Figure 1

Differential expression of primary cilia-associated proteins in the hippocampus 24 hours after neonatal *Staphylococcus epidermidis* infection. Changes are characterized by both direction and magnitude, indicating increased expression of signaling-related proteins (e.g., SLC2A1, SMAD1, SOD1, IGF1R) and decreased expression of proteins associated with cytoskeletal organization and ciliary structure (e.g., PRKAR1A, NME7, TPPP, VCL). Each panel includes the Wilcoxon rank-sum p-value, Cliff's delta, median difference, and group sample sizes.

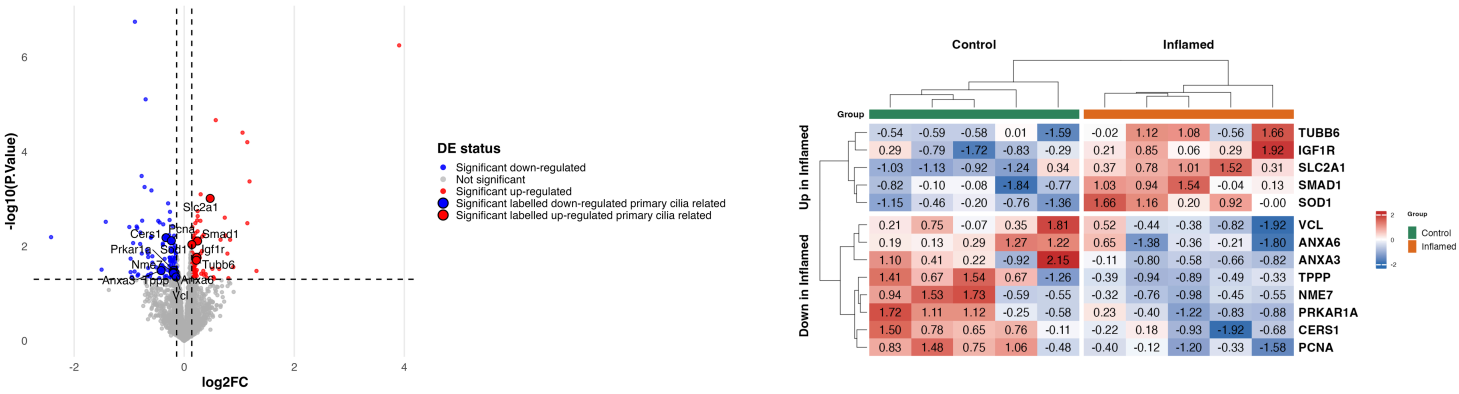


Figure 2

Differential expression of cilia-associated proteins in the hippocampus following neonatal *Staphylococcus epidermidis* infection. (A) Volcano plot showing differentially expressed proteins 24 hours after neonatal *Staphylococcus epidermidis* infection. Proteins are plotted according to $\log_2$ fold change ($\log_2$FC) and statistical significance ($-\log_{10}$ p-value). Significantly upregulated proteins are shown in red, downregulated proteins in blue, and non-significant proteins in grey. Selected cilia-associated proteins are highlighted and labeled in italics. (B) Heatmap and hierarchical clustering of differentially expressed cilia-associated proteins in control and inflamed samples. Proteins cluster into two main groups corresponding to upregulated and downregulated expression patterns in response to inflammation. Upregulated proteins (TUBB6, IGF1R, Slc2a1, SMAD1, and SOD1) show increased abundance in inflamed samples, whereas downregulated proteins (VCL, ANXA6, ANXA3, TPPP, NME7, PRKAR1A, CERS1, PCNA) show reduced expression.

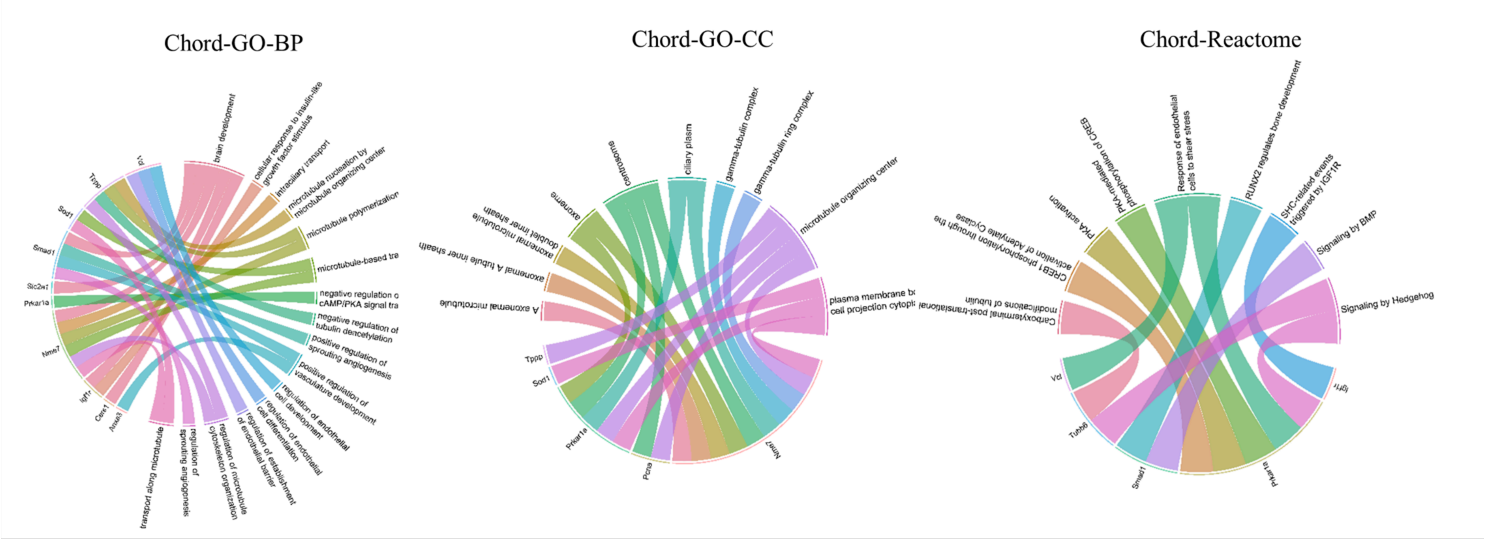


Figure 3

Integrated functional enrichment analysis of cilia-associated proteins in the hippocampus following neonatal *Staphylococcus epidermidis* infection. Left (GO-BP): Gene Ontology biological process enrichment highlights pathways related to microtubule organization, intracellular transport, cytoskeletal dynamics, and developmental signaling. Middle (GO-CC): Gene Ontology cellular component analysis shows enrichment of proteins localized to key ciliary and cytoskeletal structures, including the axoneme, centrosome, ciliary plasma, gamma-tubulin complex, and microtubule organizing center. Right (Reactome): Reactome pathway analysis reveals enrichment in signaling pathways, including cAMP/PKA signaling, CREB phosphorylation, IGF1 receptor signaling, and developmental pathways such as BMP and Hedgehog signaling. Colored links indicate the association of individual proteins with multiple biological processes, cellular compartments, and signaling pathways, demonstrating functional convergence across cilia-related molecular networks.



Figure 4

Primary cilia–related pathway enrichment in the hippocampus 24 h after *Staphylococcus epidermidis* infection. Hierarchical clustering of enriched GO terms and pathways grouped into functional clusters, highlighting microtubule organization, ciliary structures, endothelial regulation, and signaling pathways (cAMP/PKA/CREB, Hedgehog, IGF1R, BMP). Dot size indicates gene count, and color represents p-value significance.

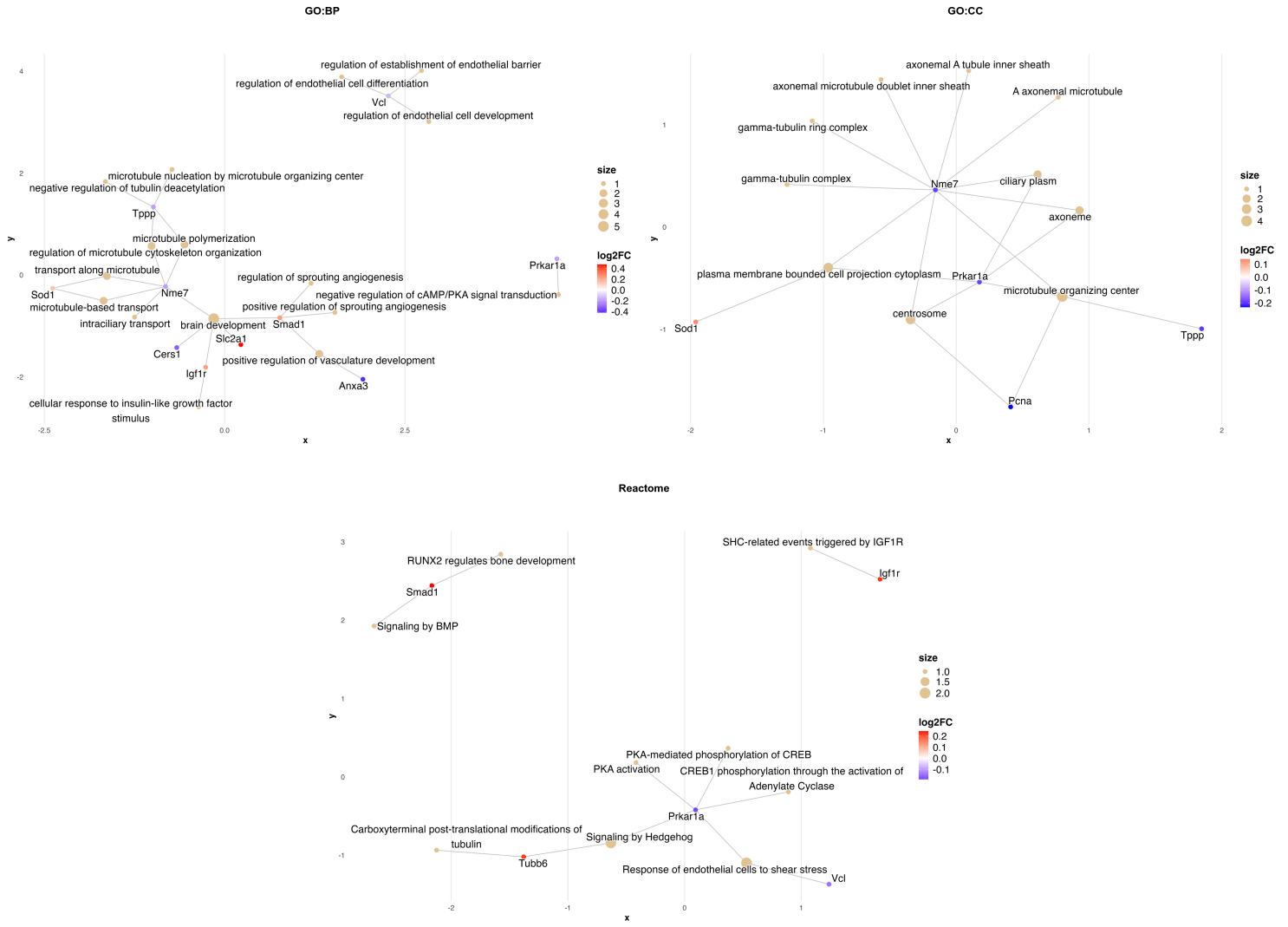


Figure 5

Gene–concept network (Cnet) analysis reveals hub proteins linking cilia-associated structural and signaling pathways in the hippocampus following neonatal *Staphylococcus epidermidis* infection. Gene–concept network (Cnet) plots showing the relationships between differentially expressed cilia-associated proteins and enriched functional categories 24 hours after neonatal *Staphylococcus epidermidis* infection. Top left (GO-BP): Network illustrating how individual proteins map to biological processes. Proteins such as *Nme7*and *Tppp* connect multiple terms related to microtubule organization and intracellular transport, while *Smad1* and *Prkar1a* show more selective associations with developmental and signaling processes. Top right (GO-CC): Network of cellular component associations demonstrating that *Nme7* acts as a central node linking multiple ciliary compartments, including axonemal structures and microtubule-organizing centers, whereas other proteins display more restricted compartmental associations. Bottom (Reactome): Network of signaling pathways showing that a limited number of proteins drive pathway enrichment, with *Prkar1a* linking cAMP/PKA and CREB signaling, *Igf1r*associated with growth factor signaling, and *Smad1* connected to BMP-related pathways. Nodes represent genes (colored by log2 fold change) or functional terms; edges indicate gene–term

associations. Node size reflects the number of connections (degree). The network highlights key hub proteins that connect multiple structural and signaling pathways.

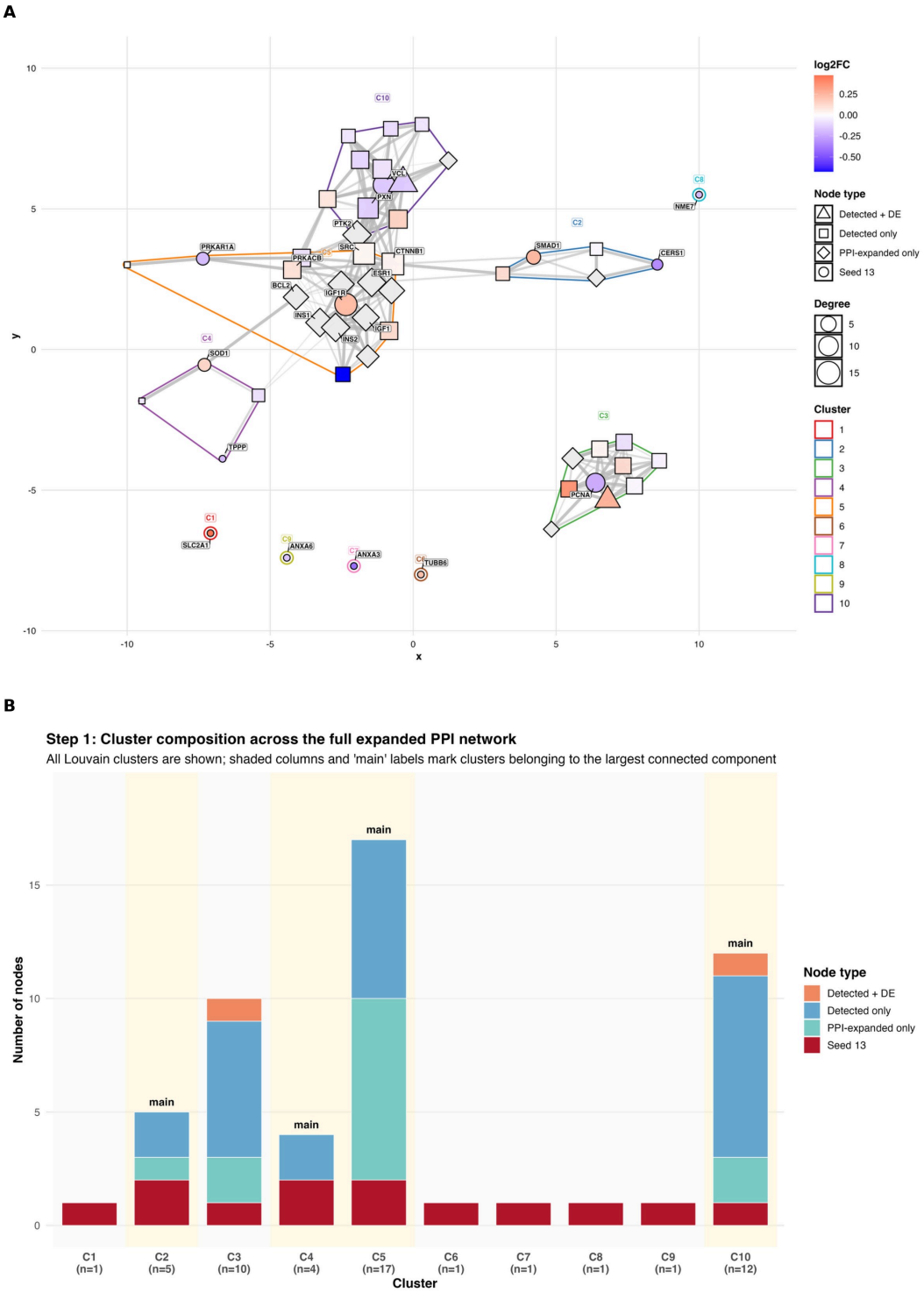


Figure 6

PPI network expansion identifies central hub proteins and cluster organization of cilia-associated proteins. (A) Protein–protein interaction (PPI) network generated from 13 primary cilia seed proteins and

top-ranked STRING partners (score ≥ 0.7). Nodes are colored by $\log_2$ fold change and shaped by category (seed proteins, detected and differentially expressed, detected only, or PPI-expanded only), with node size proportional to degree. The network reveals a densely connected central module in which proteins such as IGF1R, PRKAR1A, and CTNNB1 act as hubs linking multiple interaction partners, while peripheral clusters form smaller, functionally distinct modules. Edge colors indicate Louvain clusters, highlighting the modular organization of the expanded network. (B) Cluster composition across the expanded PPI network. Bars represent the number of nodes per cluster, stratified by node type (seed, detected and differentially expressed, detected only, or PPI-expanded only). Shaded regions denote clusters belonging to the largest connected component, illustrating that the majority of seed proteins and high-degree nodes are concentrated within the main network module, while smaller clusters consist primarily of peripheral or PPI-expanded proteins.

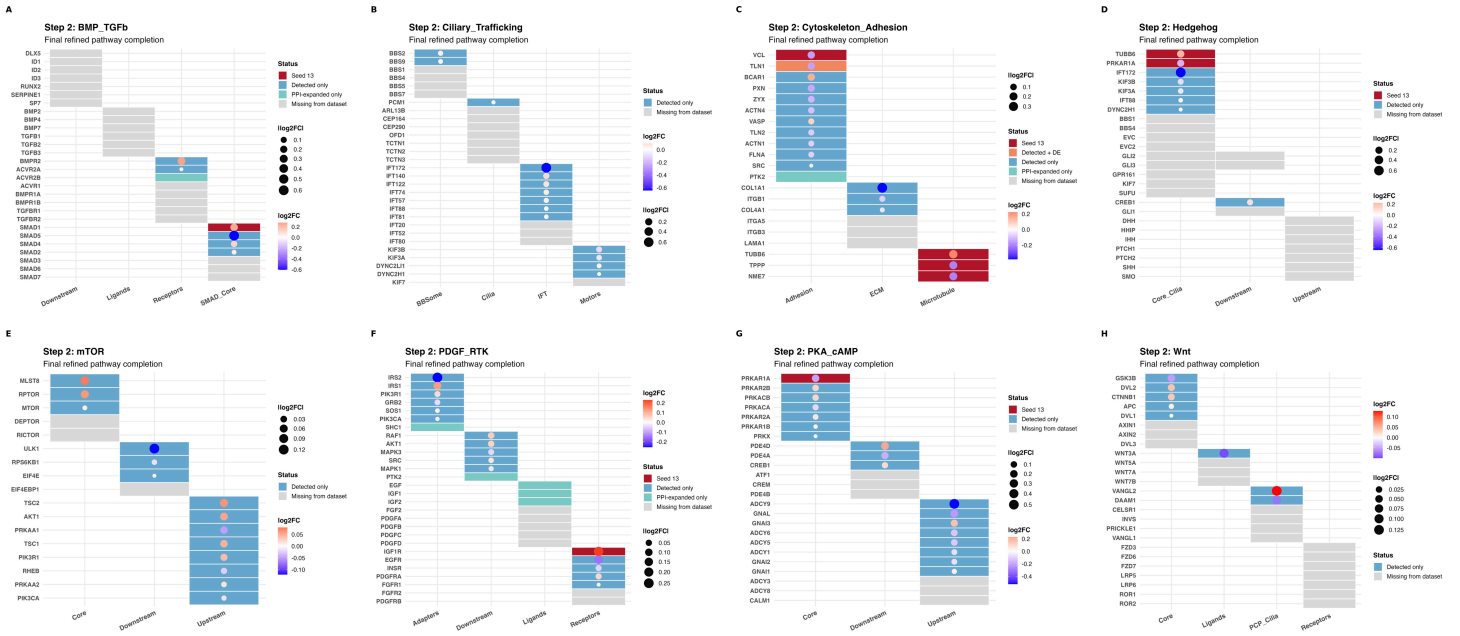


Figure 7

Pathway-level mapping of differentially abundant proteins in cilia-associated signaling pathways following postnatal infection with *SE*. (A) BMP/TGF-β signaling, (B) ciliary trafficking, (C) cytoskeleton and adhesion, (D) Hedgehog signaling, (E) mTOR signaling, (F) PDGF receptor tyrosine kinase (PDGF-RTK) signaling, (G) PKA/cAMP signaling, and (H) Wnt signaling. Each row corresponds to an individual protein, grouped by functional subcategories within each pathway (e.g., core components, upstream regulators, downstream effectors, or structural modules). Colored dots indicate the direction and magnitude of change in protein abundance, represented as log2 fold change (log2FC), with red indicating increased abundance and blue indicating decreased abundance. Dot size reflects the magnitude of change. Background color denotes protein detection status: proteins detected in the dataset, proteins identified through protein–protein interaction (PPI) expansion, and proteins not detected (missing from the dataset), as indicated in the legend.

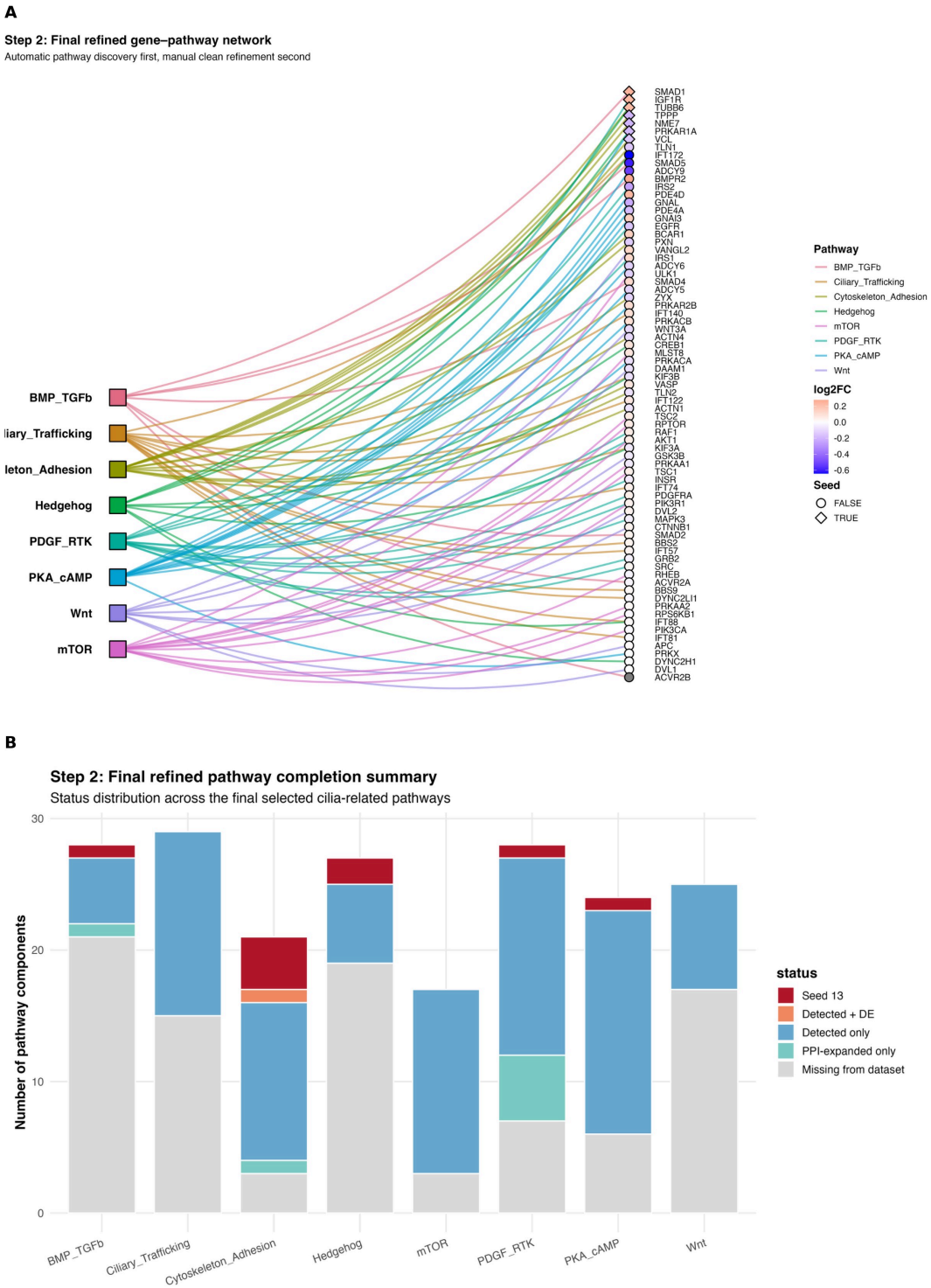


Figure 8

Integrated gene–pathway network and pathway coverage across cilia-associated signaling pathways. (A) Pathways are shown on the left, and individual proteins on the right. Lines represent associations between proteins and pathways, with colors indicating pathway membership. Node color represents log2 fold change (log2FC) in protein abundance, with red indicating increased abundance and blue indicating decreased abundance. Proteins designated as seed components are indicated accordingly. (B) Summary

of pathway component coverage across the selected pathways. Bars represent the number of proteins per pathway categorized by detection status: seed components, detected proteins (including differentially expressed proteins), detected-only proteins, proteins identified through protein–protein interaction (PPI) expansion, and proteins not detected in the dataset.

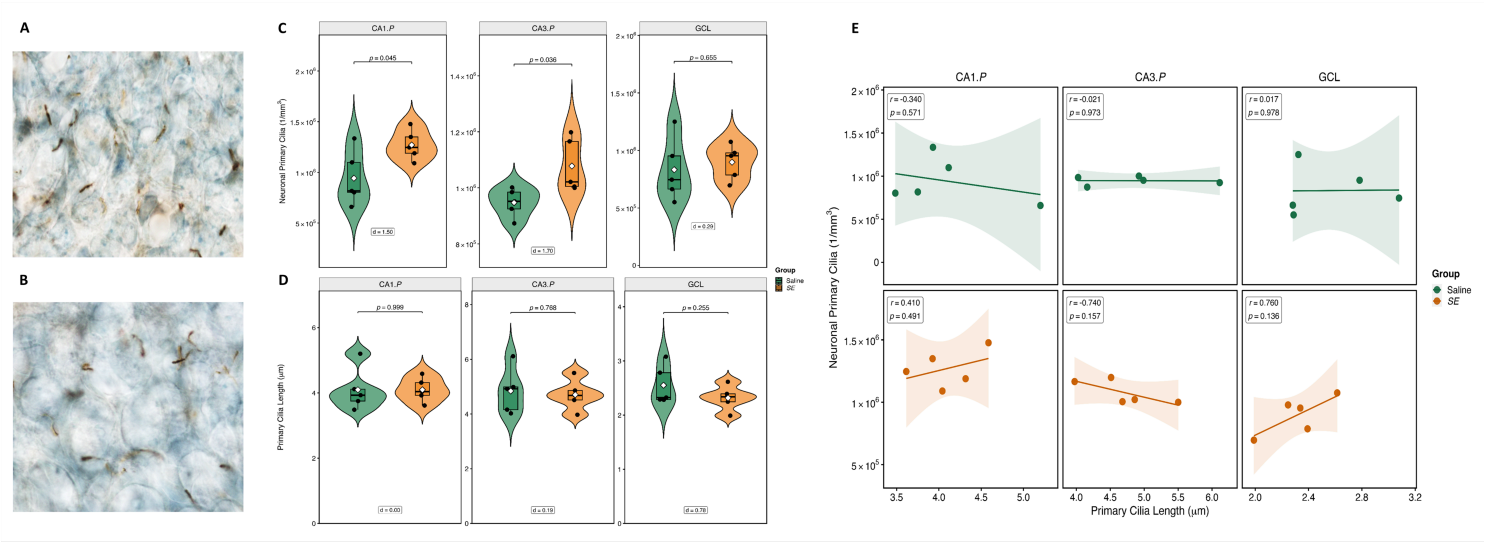


Figure 9

Legend not included with this version.

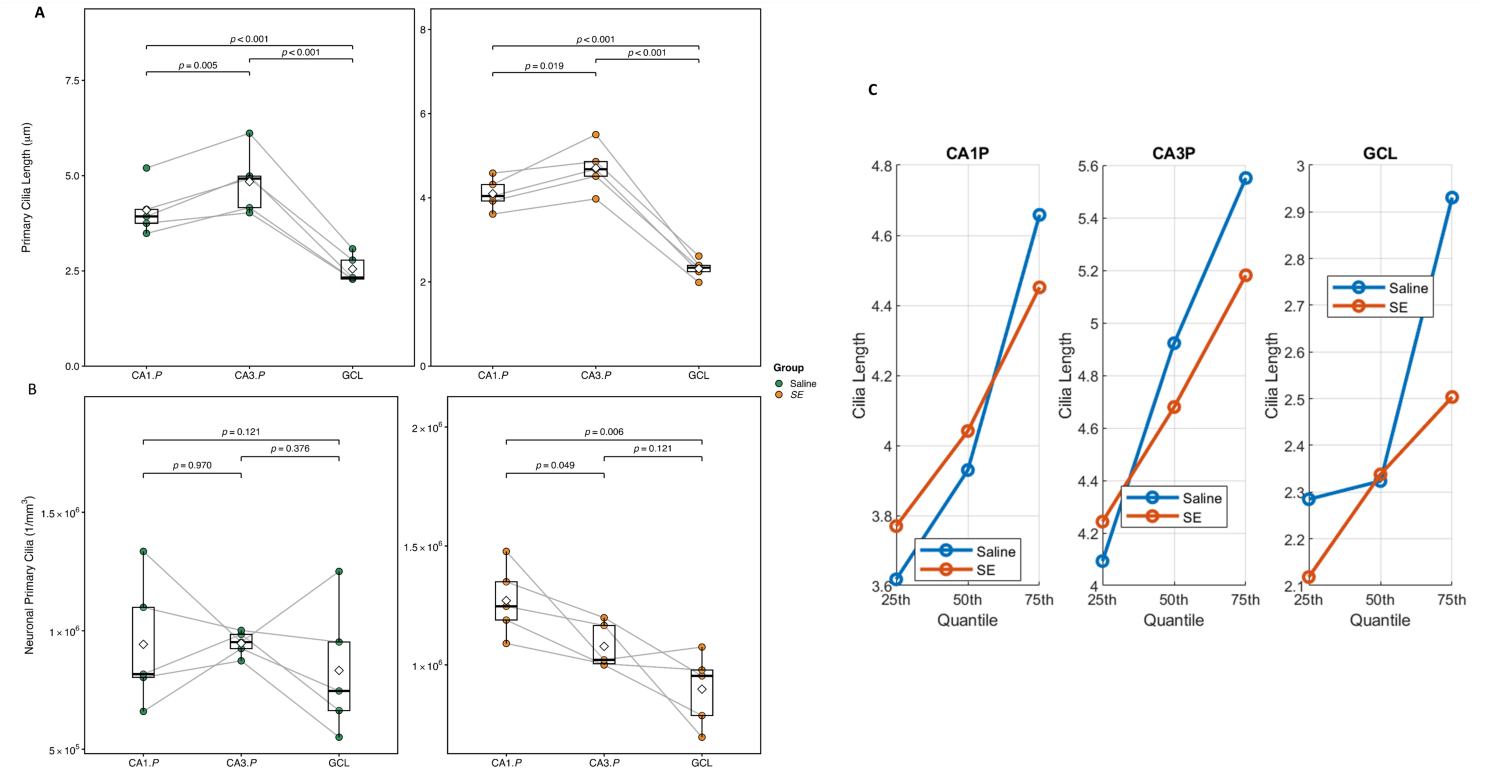


Figure 10

Legend not included with this version.

Supplementary Files

This is a list of supplementary files associated with this preprint. Click to download.

- floatimage1.png